

# Power-Law Random Banded Matrix Ensemble as the Effective Model for Many-Body Localization Transition

Wen-Jia Rao\*

*School of Science, Hangzhou Dianzi University, Hangzhou 310027, China.*

(Dated: March 30, 2022)

We employ the power-law random band matrix (PRBM) ensemble with single tuning parameter  $\mu$  as the effective model for many-body localization (MBL) transition in random spin systems. We show the PRBM accurately reproduce the eigenvalue statistics on the entire phase diagram through the fittings of high-order spacing ratio distributions  $P(r^{(n)})$  as well as number variance  $\Sigma^2(l)$ , in systems both with and without time-reversal symmetry. For the properties of eigenvectors, it's shown the entanglement entropy of PRBM displays an evolution from volume-law to area-law behavior which signatures an ergodic-MBL transition, and the critical exponent is found to be  $\nu = 0.83 \pm 0.15$ , close to the value obtained in 1D physical model by exact diagonalization while the computational cost here is much less.

## I. INTRODUCTION

The phase of matter in isolated quantum systems has attracted a lot of attention in the past decade, it is by now well-established the existence of two generic phases: an ergodic phase and a many-body localized (MBL) phase<sup>1,2</sup>. In an ergodic phase, the system acts as the heat bath for its subsystem, hence the quantum entanglement follows volume-law and exhibits ballistic spreading after quantum quench. In contrast, a MBL phase is where localization persists in the presence of weak interactions, which leads to area-law entanglement and slow entanglement spreading. The different scaling behaviors of quantum entanglement provide the modern understanding about these two phases<sup>3-11</sup>.

More traditionally, the ergodic and MBL phase are distinguished by their eigenvalue statistics<sup>12-20</sup>, whose mathematical foundation is laid by the random matrix theory<sup>21,22</sup>. The eigenvalues of an ergodic phase are well-correlated, whose distribution belongs to the Wigner-Dyson (WD) class which further divides into three ensembles depending on the system's symmetry: the Gaussian orthogonal/unitary ensemble (GOE/GUE) for orthogonal/unitary systems with/without time reversal symmetry, and Gaussian symplectic ensemble (GSE) for time-reversal invariant systems with broken spin rotational invariance. On the contrary, the eigenvalues in MBL phase are independent of each other and belongs to the Poisson ensemble.

Compared to the properties of each phase, much less is known about the evolution in between. Up to now, there have been a number of proposed random matrix models accounting for the spectral statistics right at the critical point, or even along the whole phase diagram<sup>23-30</sup>, among which two outstanding models are the Gaussian  $\beta$  ensemble<sup>29</sup> and the  $\beta - h$  model<sup>30</sup>. The former generalizes the WD classes into the one with continuous Dyson index  $\beta \in (0, \infty)$ , and is shown to faithfully reproduce the short-range level correlations for the MBL system, but the deviations soon become non-negligible when long-range correlations are considered. On the other hand, the two-parameter  $\beta - h$  model is shown to accurately describe the level correlations on both short and long ranges during MBL transition. However, this model is based on the joint probability distribution of eigenvalues and lacks clear

matrix construction, hence cannot provide insights about the eigenvectors.

Given above facts, we impose three basic requirements for an optimal effective model for an MBL system: (i) it should accurately reproduce the eigenvalue statistics of the physical model – on both short and long ranges – on the entire phase diagram; (ii) it should have well-defined matrix construction, whose eigenvectors should further reflect the universal properties of physical system, such as the scaling of entanglement; (iii) it should contain as less tuning parameters as possible.

In this work, we employ the power-law random banded matrix (PRBM)<sup>31</sup> with fixed  $B = 1$  and single tuning parameter  $\mu$  (definitions come in next section) as the effective model for studying MBL transition. PRBM was introduced as the critical random matrix model for Anderson localization transition, which contains all the key features of the latter such as multifractality of eigenvectors and spectrum compressibility, as verified in a considerable number of works<sup>32-40</sup>. And here, we bring PRBM to the many-body regime. Remarkably, we find nearly perfect agreement for the eigenvalue statistics between the single-parameter PRBM and typical physical models over the entire phase diagram, in cases both with and without time-reversal symmetry. Moreover, for the eigenvectors, we find PRBM holds both volume-law and area-law behavior for its entanglement entropy (EE), which signatures an ergodic-MBL transition, and the critical exponent is found to be  $\nu = 0.83 \pm 0.15$ , close to that obtained by exact diagonalization for physical model<sup>41</sup> while the computational cost here is much less.

This paper is organized as follows. In Sec.II we introduce the PRBM. In Sec.III we use PRBM to fit the eigenvalue statistics of typical physical models, both with and without time-reversal symmetry. In Sec.IV we study the entanglement scaling in PRBM, and determine the corresponding critical exponent. Discussion and conclusion come in Sec.V.

## II. POWER-LAW RANDOM BANDED MATRIX

The power-law random banded matrix (PRBM) ensemble<sup>31</sup> is a Gaussian ensemble of  $N \times N$  dense Hermitian matrices

$H$  with random elements, whose distribution satisfy

$$\begin{aligned} \langle H_{ij} \rangle &= 0, \quad \langle (H_{ii})^2 \rangle = \beta^{-1}, \\ \langle (H_{ij}^\alpha)^2 \rangle &= \beta^{-1} \left[ 1 + (|j-i|/B)^{2\mu} \right]^{-1}, \quad \alpha = 1, 2, \dots, \beta \end{aligned} \quad (1)$$

where  $\beta = 1, 2, 4$  is the Dyson index,  $H_{ij}^\alpha$  is the  $\alpha$ -th component of the non-diagonal element  $H_{ij}$ . For instance, in the unitary PRBM with  $\beta = 2$ ,  $H_{ij}^1$  and  $H_{ij}^2$  are the real and imaginary part of  $H_{ij}$ . PRBM is controlled by the tuning parameter  $\mu \in (0, \infty)$ : in the limit  $\mu \rightarrow 0$ , we have  $\langle (H_{ij}^\alpha)^2 \rangle \rightarrow 1$ , hence  $H$  becomes the standard random matrix in WD classes for the ergodic phases; while in the limit  $\mu \rightarrow \infty$ , we have  $\langle (H_{ij}^\alpha)^2 \rangle \rightarrow 0$  for  $i \neq j$ , which means all non-diagonal elements vanish and  $H$  becomes a random diagonal matrix for the Poisson ensemble. In cases with  $B \gg 1$  and  $B \ll 1$ , the critical point is analytically proved to be  $\mu_c = 1$ , separating the metallic ( $\mu < 1$ ) and localized ( $\mu > 1$ ) phase in the Anderson model<sup>31-33</sup>. In this work, we concentrate on the case with  $B = 1$  which is by far inaccessible by analytical treatment and leave  $\mu$  as the single varying parameter. The criticality of  $\mu_c = 1$  in this case has been numerically verified in earlier works<sup>39,42</sup>, and will be further justified in this study.

The well-defined matrix construction of PRBM allows us to numerically study both its eigenvalues and eigenvectors, and we start with the former. As the first step, we show PRBM ( $B = 1$ ) with varying  $\mu$  can describe the interpolation between WD and Poisson. Specifically, we numerically diagonalize 400 samples of PRBM at various  $\mu$ s, with the matrix dimension  $N = 2000$ , and take 400 eigenvalues in the middle to determine eigenvalue statistics. For the latter, we study the distribution of spacing ratios, whose definition is<sup>12</sup>

$$r_i^{(n)} = \frac{E_{i+2n} - E_{i+n}}{E_{i+n} - E_i}. \quad (2)$$

The form of  $P(r^{(n)})$  with  $n = 1$  has been analytically derived in Ref. [43] and later generalized to higher-order ones to incorporate level correlations on longer ranges<sup>44,45</sup>. Compared to the more traditional quantities like level spacings  $\{s_i = E_{i+1} - E_i\}$  or number variance  $\Sigma^2(l)$ , spacing ratios are independent of density of states and requires no unfolding procedure, which is non-unique and may raise subtle misleading signatures in certain system<sup>46</sup>.

As the first demonstration, we plot  $P(r^{(1)})$  of PRBM with varying  $\mu$  in cases with  $\beta = 1, 2$ . Particularly, we aim at three target distributions: WD for ergodic phase; Poisson for MBL phase; and that of short-range plasma model (SRPM)<sup>25</sup> with semi-Poisson distribution, which is commonly believed to be the critical distribution at the ergodic-MBL transition point<sup>24,28</sup>. The expressions of them are<sup>25,26,43</sup>

$$P(r) = \begin{cases} Z_\beta \frac{(r+r^2)^\beta}{(1+r+r^2)^{1+3\beta/2}}, & \text{WD;} \\ Z'_\beta \frac{r^\beta}{(1+r)^{2(\beta+1)}}, & \text{SRPM;} \\ \frac{1}{(1+r)^2}, & \text{Poisson.} \end{cases} \quad (3)$$

where  $Z_\beta$  and  $Z'_\beta$  are normalization factors. The fittings results are in Fig. 1, as can be seen, PRBM with  $\mu = 0.7, 1.08, 2$

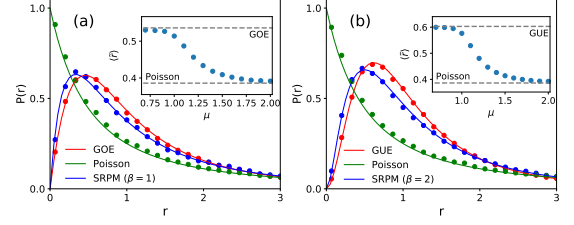


FIG. 1.  $P(r)$  in (a) orthogonal and (b) unitary PRBM, where the red, blue, green dots stand for  $\mu = 0.7, 1.08, 2$  in both sub-figures. Insets: Evolution of  $\langle \tilde{r} \rangle$  in respective cases.

accurately reproduce the three target distributions in both orthogonal and unitary cases.

To further illustrate the level evolution, we compute the average value of a variant spacing ratios<sup>12</sup>, which is  $\tilde{r}_i = \frac{\min\{s_{i+1}, s_i\}}{\max\{s_{i+1}, s_i\}}$ .  $\langle \tilde{r} \rangle$  takes different values in each ensemble<sup>43</sup>, namely  $\langle \tilde{r} \rangle_{\text{GOE}} = 0.536$ ,  $\langle \tilde{r} \rangle_{\text{GUE}} = 0.603$  and  $\langle \tilde{r} \rangle_{\text{Poisson}} = 0.386$ . As shown in the insets of Fig. 1, PRBM faithfully describes the continuous interpolation between WD and Poisson. As the next step, we use PRBM to fit the eigenvalue statistics of physical models, with particular attention paid for long-range level correlations.

### III. FITTING EIGENVALUE STATISTICS

We first consider the paradigmatic orthogonal spin model with ergodic-MBL transition, that is, the anti-ferromagnetic Heisenberg model with random external fields<sup>47</sup>, the Hamiltonian reads

$$H_0 = \sum_{i=1}^L \mathbf{S}_i \cdot \mathbf{S}_{i+1} + h \sum_{i=1}^L \varepsilon_i S_i^z, \quad (4)$$

The anti-ferromagnetic coupling strength is set to be 1, and  $\varepsilon_i$ s are random variables within range  $[-1, 1]$ . This Hamiltonian commutes with  $S_T^z = \sum_i S_i^z$  and allows us to reach larger systems by focusing on one sector. In this work, we choose  $L = 16$  in the  $S_T^z = 0$  sector, with Hilbert space dimension  $C_{16}^8 = 12870$ . We exactly diagonalize  $H_0$  at various random strengths with 400 samples taken at each point, and select 400 eigenvalues in the middle to determine  $P(r^{(n)})$ .

This physical model displays an ergodic-MBL evolution in the range  $h \in (1, 5)$ , we select several representative points over the entire phase diagram, and compared the resulting  $P(r^{(n)})$  to those of PRBM with fitted parameter  $\mu$ , the results are shown in Fig. 2(a)-(e). Remarkably, we observe nearly perfect agreements between PRBM and physical model in all the cases considered. For clarity we only display the fitting results up to  $n = 5$  in Fig. 2(a)-(e), while the agreements maintain up to much longer ranges even in the transition region ( $h \in (2, 3)$  in this system length).

To further study the long-range level correlations, we employ the number variance  $\Sigma^2(l)$ <sup>21,22</sup>. Unlike spacing ratios,  $\Sigma^2(l)$  is very sensitive to the concrete unfolding strategy, and

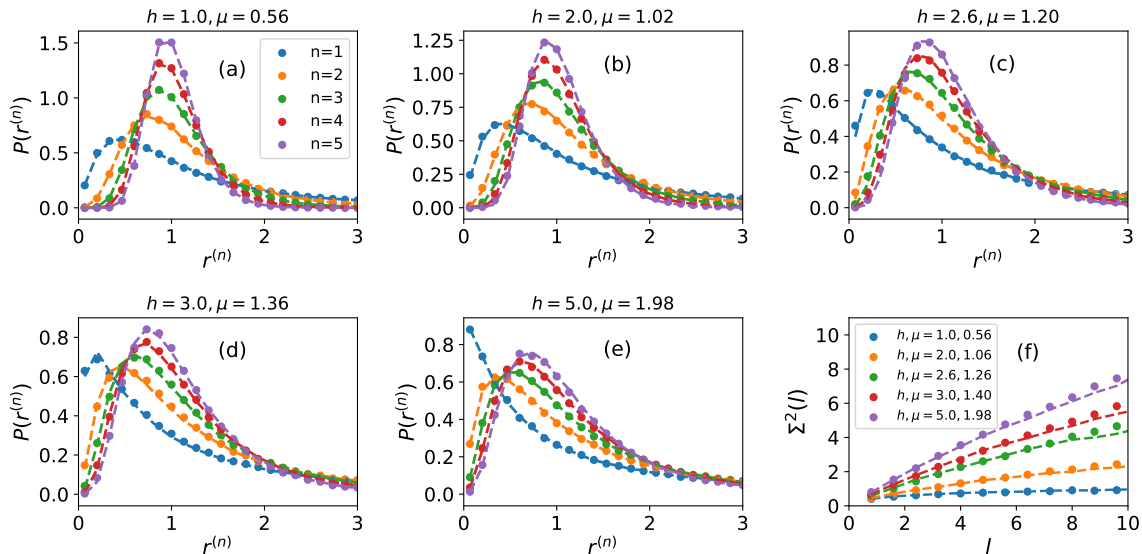


FIG. 2. (a)-(e) Comparisons of the spacing ratio distributions  $P(r^{(n)})$  up to  $n = 5$  between the orthogonal spin model with various disorder strengths and PRBM with  $\beta = 1$ , where the title of each sub-figure indicates the disorder strength  $h$  and fitted  $\mu$ . (a)-(e) share the same legend. (f) Evolution of number variance  $\Sigma^2(l)$  of the physical model and PRBM, the fitted  $\mu$ s are displayed in the figure legend. The values of  $\mu$  fitted by  $P(r^{(n)})$  and  $\Sigma^2(l)$  match perfectly in the ergodic ( $h = 1$ ) and MBL ( $h = 5$ ) phase, and their deviations in the transition region ( $h = 2 \sim 3$ ) are kept within 5%.

here we used the normal unfolding with third-order polynomials. Fig. 2(f) displays the results, where the optimal  $\mu$ s of PRBM are independently fitted through  $\Sigma^2(l)$ . Again, we observe very good agreements. Notably, the optimal values of  $\mu$  fitted by  $P(r^{(n)})$  and  $\Sigma^2(l)$  match perfectly for cases deep in the ergodic ( $h = 1$ ) and MBL ( $h = 5$ ) phase, and the relative deviations in the transition region are kept within 5% – a satisfying accuracy.

We stress here the fittings of high-order spacing ratios  $P(r^{(n)})$  with  $n > 1$  and  $\Sigma^2(l)$  are necessary, since it is known that different random matrix models may have very similar local level statistics<sup>48,49</sup>. For example, the Brownian ensemble (linear combination of random matrix in WD and Poisson ensemble) and the Gaussian  $\beta$  ensemble are both capable of describing  $P(r^{(n)})$  with  $n = 1$  for the ergodic-MBL transition, but their difference soon become non-negligible when higher-order spacing ratios are considered<sup>27</sup>.

To illustrate the power of PRBM in the unitary ( $\beta = 2$ ) case, we break the time-reversal symmetry of  $H_0$  in Eq. (4) by adding a term  $JH_1$ , where<sup>13</sup>

$$H_1 = \sum_{i=1}^{L-2} \mathbf{S}_i \cdot (\mathbf{S}_{i+1} \times \mathbf{S}_{i+2}), \quad (5)$$

and we fix  $J = 0.2$  without loss of generality. This model also preserve  $S_T^z$ , and we likewise study in the  $S_T^z = 0$  sector of an  $L = 16$  system, with the rest settings identical to the previous model. The fittings of  $P(r^{(n)})$  and  $\Sigma^2(l)$  by PRBM in various disorder strengths are collected in Fig. 3(a)-(e) and (f) respectively. Once again, we observe nearly perfect agreements between PRBM and physical data in all cases. The deviations

are slightly larger than the orthogonal case in the intermediate region, suggesting a larger finite size effect, this situation also happen in models without  $S_T^z$  conservation (see the appendix).

It is worth mentioning that the representative randomness strengths are deliberately selected. To be specific, the ergodic-MBL transition point in all these spin systems have been studied in Ref. [26], and we correspondingly select five points to represent the “entire phase diagram”, i.e. the cases deep in the ergodic/MBL phases, right at the transition point, and intermediate between the ergodic/MBL phases and transition point. We believe that such choices are sufficient to represent the whole phase diagram.

Up to now, we have verified the validity of PRBM in modeling the eigenvalue statistics of physical systems both with and without time-reversal symmetry. We can further show this is not model-dependent by fitting physical models without  $S_T^z$  conservation, which is presented in the appendix. Next we turn to the study of eigenvectors.

#### IV. SCALING OF ENTANGLEMENT ENTROPY

The eigenvector of PRBM is a bit tricky since it lacks a direct correspondence to physical observables. Nevertheless, we can artificially view  $H$  as the Hamiltonian matrix for a system of fictitious local degrees of freedoms, then we are able to study the general quantities of eigenvectors. Here we consider the quantity of modern interest, that is, the entanglement entropy (EE). In this section we focus on the orthogonal PRBM with  $\beta = 1$ .

To get the EE of PRBM, we treat  $H$  with dimension  $N \times N$

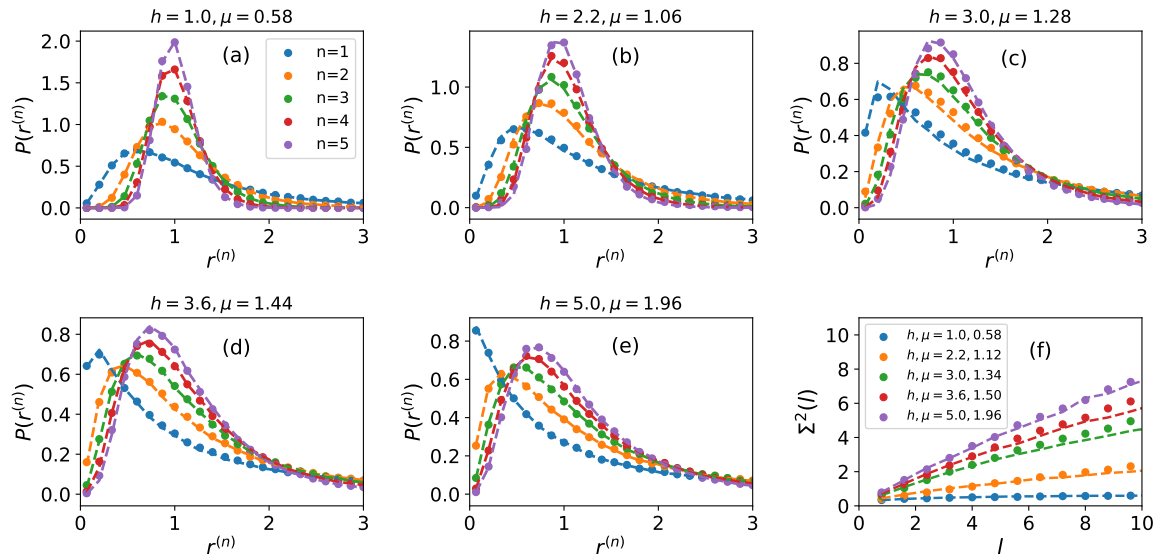


FIG. 3. (a)-(e) Spacing ratio distributions  $P(r^{(n)})$  in the unitary spin model without time-reversal symmetry and PRBM with  $\beta = 2$ , the randomness strength  $h$  and fitted  $\mu$  are displayed in the title of each sub-figure. (f) Evolution of number variance  $\Sigma^2(l)$  of the physical model and PRBM with fitted  $\mu$ s displayed in the figure legend. Dots and lines stand for physical data and PRBM in all cases.

as the Hamiltonian describing the interaction between  $L_f$  fictitious spin-1/2s, where  $L_f = \log_2 N$ . A typical eigenvector  $|\varphi\rangle$  is therefore represented by an  $N$ -dimensional column vector. Then by dividing the system into equal halves A and B with  $L_f/2$  spins,  $|\varphi\rangle$  is decomposed as  $|\varphi\rangle = \sum_{ij} \varphi_{ij} |\varphi_A\rangle_i |\varphi_B\rangle_j$  where  $|\varphi_A\rangle_i$  and  $|\varphi_B\rangle_j$  are both  $\sqrt{N}$ -dimensional column vectors representing the subsystem's basis and  $\varphi_{ij}$  is obtained by reshaping the  $N$ -dimensional column vector  $|\varphi\rangle$  into a  $\sqrt{N} \times \sqrt{N}$  matrix  $\varphi$ . The reduced density matrix  $\rho_A = \text{Tr}_B(|\varphi\rangle\langle\varphi|)$  is thus equal to  $\varphi\varphi^\dagger$  and EE is obtained through  $S = -\text{Tr}_A(\rho_A \log \rho_A)$ .

We compute the EE averaged among the middle 200 eigenvectors of  $H$  with parameter  $\mu$ , and determine its scaling with the fictitious system length  $L_f$ , the results are in Fig 4(a). We see that for  $\mu$  in the ergodic phase,  $S$  grows linearly with  $L_f$ , which reflects the volume-law behavior; while for large  $\mu$ , EE saturates to a small value, reflecting the area-law behavior in an one-dimensional MBL phase.

We then draw the evolution of  $S$  divided by the Page value  $S_P = 0.5(L_f \log(2) - 1)$  for a pure random state<sup>50</sup> as a function of parameter  $\mu$ , the results are shown in Fig 4(b). As expected,  $S/S_P$  decreases from 1 in ergodic phase to 0 for MBL phase with increasing  $\mu$ . The curves with different matrix dimensions  $N$  cross at the critical point  $\mu_c \simeq 1$ , confirming the criticality in this case.

We further zoom in the transition region to determine the critical exponent by assuming  $S/S_P = g((\mu - \mu_c) L_f^{1/\nu})$ , with  $g$  being an unspecified continuous function. The finite-size collapse is shown in the inset of Fig. 4(b), where we find  $\mu_c = 1.02 \pm 0.03$  and  $\nu = 0.83 \pm 0.15$ . This value of  $\nu$  is smaller, while close to the one  $\nu \sim 1$  found by exact diagonalizations for the orthogonal spin model in Eq. (4)<sup>41</sup>, which

supports the validity of PRBM in modeling the eigenvectors of physical system.

It's worth emphasizing that the maximal matrix dimension in Fig. 4 is  $N = 6400$ , which is much smaller than the spin model in Ref. [41] (up to  $L = 18$  with  $\dim(H) = 48620$ ). This fact strongly hints the universal properties of MBL transition is highly distilled in the power-law construction of PRBM. This is of course far from being fully understood, and further insights can be gained by constructing a physical model whose Hamiltonian bears the form of PRBM, which is left for a future study.

## V. CONCLUSION AND DISCUSSION

In this work, we aim to search for an effective mathematical model that can phenomenologically describe the ergodic-MBL transition in physical spin models. We showed that the PRBM with fixed  $B = 1$  and single tuning parameter  $\mu$  is such a proper choice. For one side, we show that PRBM gives nearly perfect description for the eigenvalue statistics – both on short and long ranges – on the entire phase diagram with ergodic-MBL transition, in systems both with and without time-reversal symmetry. Moreover, for the eigenvectors, it's shown the EE of PRBM displays an evolution from volume-law to area-law behavior which signatures an ergodic-MBL transition, and the critical exponent is found to be  $\nu = 0.83 \pm 0.15$ , close to the value obtained by exact diagonalization in physical model. To the best of our knowledge, PRBM is the first single-parameter random matrix model that models both the eigenvalues and eigenvectors of disordered physical systems.

It's remarkable that the PRBM with simple construction

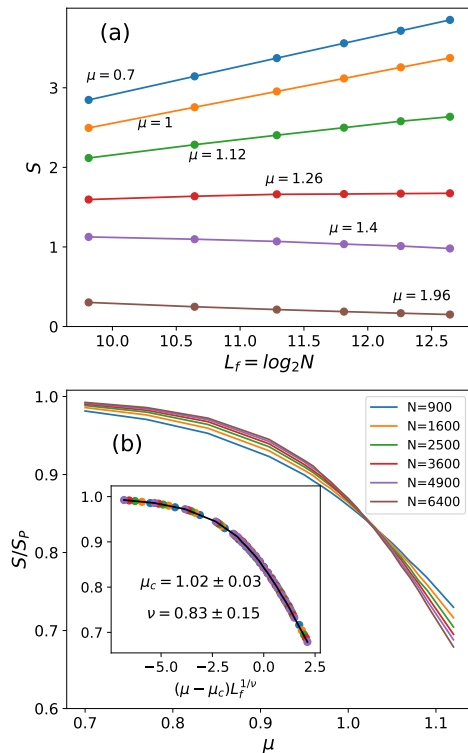


FIG. 4. (a) Average half-chain EE with respect to fictitious system length  $L_f$  in PRBM with different  $\mu$ s. (b) Evolution of EE  $S$  divided by the Page value  $S_P$ , a crossing indicates a critical point at  $\mu \sim 1$ . For eye’s convenience to observe the crossing, data for larger  $\mu$  are omitted. Inset: Finite-size collapse for  $S/S_P$  near the critical region, the estimated critical point  $\mu_c$  and critical exponent  $\nu$  are displayed.

and single parameter can model both the eigenvalues and eigenvectors of a physical system, which suggests the universal, model-independent physics of MBL system is highly distilled in PRBM. One way to interpret this result is to view PRBM as the late-stage matrix during the renormalization flow that diagonalize the Hamiltonian<sup>51–54</sup>, where the diagonal and off-diagonal elements represent eigenenergies of the local-integral-of-motions (LIOMs) and the interactions between them. Actually, hints for such a power-law interaction between LIOMs have already been noticed in Ref. [54]. Another approach is to view MBL as the single particle Anderson localization in the Fock space<sup>55,56</sup>, where the diagonal and off-diagonal elements stand for the Hattree-Fock and hopping terms. It is an interesting question to construct a corresponding physical model in this regard.

A noticeable property of PRBM is that it’s dense, while in most physical systems with finite interaction range the Hamiltonian matrix is highly sparse. It’s then natural to ask whether the sparsity should be taken into account when construct-

ing an effective random matrix model. Such a question has been attempted in Ref.[57], where the authors constructed the “scaffolding” random matrix ensemble that is much sparser than PRBM for the metal-insulator transition in interacting Fermionic system. It’s an interesting question whether the scaffolding random matrix can describe the spectral evolution as accurately as PRBM does. On the other hand, given the efficiency of PRBM in describing the unitary spin systems with next-nearest neighboring interaction (Fig. 3) and with only nearest neighboring interaction (Fig. 6 in the appendix), it’s tempting to conclude that the interaction range does not affect the level evolution. However, we also note a recent work that studies the Haldane-Shastry model with infinite interaction range, where the authors claimed the spectral statistics is neither WD nor Poissonian even when the randomness is very large<sup>58</sup>. Therefore, the effect of increasing interaction range remains to be explored.

The most interesting results are the entanglement behaviors in Sec.IV. The results in Fig. 4(a) indicate that PRBM contains an area-law to volume-law transition that hints an ergodic-MBL transition, while the physical correspondence of the auxiliary bipartition is still unclear since PRBM has no direct sense of space or locality. In other words, it’s not clear whether such an auxiliary bipartition is more close to the normal left-right bipartition or the “comb bipartition” (an extensive bipartition of system into alternating subsystems)<sup>59,60</sup>. Although the critical exponent  $\nu$  extracted in Fig. 4(b) supports the former, a detailed evaluation is possible only if we find a physical model whose Hamiltonian bears the form of PRBM. We also do not discuss the existence of weak ergodicity breaking of the PRBM in the range  $0.5 < \mu < 1$ <sup>61–63</sup>, which may not affect the spectral statistics but have important influence on the eigenvector structures.

The construction of PRBM relies only on symmetry, regardless of the type of randomness. Therefore, it’s natural to ask whether it can describe the Griffiths effect, which distinguishes the MBL induced by random disorder from that by quasi-periodic potential. It is suggested<sup>28,41</sup> the existence of Griffiths regime can be revealed by the peak of sample-to-sample variance  $V_S$  of the mean spacing ratio  $\langle \tilde{r} \rangle$ , which is, however, absent in the PRBM. A possible way to induce the peak of  $V_S$  is to construct a linear combination of PRBMs with different  $\mu$ s<sup>28</sup>, which unavoidably introduces extra parameters. Therefore, a single-parameter random matrix model accounting for the Griffiths regime remains to be explored.

We expect that our work paves the way to the understanding of MBL and related systems in several ways. First, our model is the first single-parameter random matrix model that reproduces both the short and long range eigenvalue statistics of an MBL system, which makes the quantitative description for the evolution between ergodic and MBL phase possible. Second, there is an existing discrepancy on the value of critical exponent  $\nu$  obtained by exact diagonalization and renormalization group<sup>41,64</sup>, it is then attracting to perform certain renormalization to the PRBM, which may help to resolve this debate. Last but not least, we have also computed the EE in the unitary PRBM, and we observe totally similar scaling behaviors and critical exponent to the orthogonal PRBM, we

note similar results have been noted in Ref.[42]. This hints the critical property of the unitary spin model is also similar to the orthogonal model. Understanding the effect of system's symmetry on MBL transition is certainly an important task, and we left it to a future study.

## VI. ACKNOWLEDGEMENTS

The author acknowledges M. Haque and I. Khaymovich for stimulating and helpful discussions. This work is supported by the National Natural Science Foundation of China through Grant No.11904069.

**Data Availability Statement:** The data that support the figures within this paper are available from the corresponding author upon reasonable request.

### Appendix A: Fitting Spin Models without $S_T^z$ conservation

In this section we use PRBM to fit the eigenvalue statistics of random spin models without  $S_T^z$  conservation, the Hamil-

tonian is as follows

$$H = \sum_{i=1}^L \mathbf{S}_i \cdot \mathbf{S}_{i+1} + \sum_{i=1}^L \sum_{\alpha=x,y,z} h^\alpha \varepsilon_i^\alpha S_i^\alpha. \quad (\text{A1})$$

We will also consider the cases both with and without time-reversal symmetry. For the former, it is the case with  $h^x = h^z = h \neq 0$  and  $h^y = 0$ ; while for the latter, it is  $h^x = h^y = h^z = h \neq 0$ . For both models we simulate an  $L = 13$  system, with Hilbert space dimension  $2^{13} = 8192$ . In all cases, the number of eigenvalue spectrum samples is 400, and we take 400 eigenvalues in the middle to determine  $P(r^{(n)})$ .

For the orthogonal case, we likewise take several representative randomness strengths to determine spacing ratio distributions  $P(r^{(n)})$  and number variance  $\Sigma^2(l)$ , and compare them to those of orthogonal PRBM with  $\beta = 1$ , the results are collected in Fig. 5. This model suffers less from finite-size effect, hence the fittings are close to perfect. Moreover, the optimal parameter  $\mu$  fitted by  $P(r^{(n)})$  and  $\Sigma^2(l)$  are very close in most of the phase diagram, except for the transition region  $h \sim 3$ , as can be viewed from the last sub-figure of Fig. 5.

For the time-reversal breaking case with  $h^x = h^y = h^z = h$ , the fitting results are displayed in Fig. 6. The finite size effects are slightly larger than the orthogonal case, just like in the models with  $S_T^z$  conservation as discussed in the main text. Nevertheless, the deviations between the values of  $\mu$  fitted by  $P(r^{(n)})$  and  $\Sigma^2(l)$  are still less than 5%.

\* wjr@hdu.edu.cn

- <sup>1</sup> I. V. Gornyi, A. D. Mirlin, and D. G. Polyakov, Phys. Rev. Lett. **95**, 206603 (2005); **95**, 046404 (2005).
- <sup>2</sup> D. M. Basko, I. L. Aleiner, and B. L. Altshuler, Ann. Phys. **321**, 1126 (2006).
- <sup>3</sup> J. A. Kjall, J. H. Bardarson, and F. Pollmann, Phys. Rev. Lett. **113**, 107204 (2014).
- <sup>4</sup> Z. C. Yang, C. Chamon, A. Hama, and E. R. Mucciolo, Phys. Rev. Lett. **115**, 267206 (2015).
- <sup>5</sup> M. Serbyn, A. A. Michailidis, M. A. Abanin, and Z. Papić, Phys. Rev. Lett. **117**, 160601 (2016).
- <sup>6</sup> J. Gray, S. Bose, and A. Bayat, Phys. Rev. B **97**, 201105 (2018).
- <sup>7</sup> M. Serbyn, Z. Papić, and D. A. Abanin, Phys. Rev. X **5**, 041047 (2015).
- <sup>8</sup> H. Kim and D. A. Huse, Phys. Rev. Lett. **111**, 127205 (2013).
- <sup>9</sup> M. Znidaric, T. Prosen, and P. Prelovsek, Phys. Rev. B **77**, 064426 (2008).
- <sup>10</sup> J. H. Bardarson, F. Pollman, and J. E. Moore, Phys. Rev. Lett. **109**, 017202 (2012).
- <sup>11</sup> M. Serbyn, Z. Papić, and D. A. Abanin, Phys. Rev. B **90**, 174302 (2014).
- <sup>12</sup> V. Oganesyan and D. A. Huse, Phys. Rev. B **75**, 155111 (2007).
- <sup>13</sup> Y. Avishai, J. Richert, and R. Berkovits, Phys. Rev. B **66**, 052416 (2002).
- <sup>14</sup> N. Regnault and R. Nandkishore, Phys. Rev. B **93**, 104203 (2016).
- <sup>15</sup> S. D. Geraedts, R. Nandkishore, and N. Regnault, Phys. Rev. B **93**, 174202 (2016).
- <sup>16</sup> V. Oganesyan, A. Pal, D. A. Huse, Phys. Rev. B **80**, 115104 (2009).

- <sup>17</sup> A. Pal, D. A. Huse, Phys. Rev. B **82**, 174411 (2010).
- <sup>18</sup> S. Iyer, V. Oganesyan, G. Refael, D. A. Huse, Phys. Rev. B **87**, 134202 (2013).
- <sup>19</sup> D. J. Luitz, N. Laflorencie, and F. Alet, Phys. Rev. B **91**, 081103(R) (2015).
- <sup>20</sup> C. L. Bertrand and A. M. García-García, Phys. Rev. B **94**, 144201 (2016).
- <sup>21</sup> M. L. Mehta, *Random Matrix Theory*, Springer, New York (1990).
- <sup>22</sup> F. Haake, *Quantum Signatures of Chaos*, (Springer 2001).
- <sup>23</sup> P. Shukla, New Journal of Physics **18**, 021004 (2016).
- <sup>24</sup> M. Serbyn and J. E. Moore, Phys. Rev. B **93**, 041424(R) (2016).
- <sup>25</sup> E. B. Bogomolny, U. Gerland and C. Schmit, Eur. Phys. J. B **19**, 121 (2001).
- <sup>26</sup> W.-J. Rao, J. Phys. A: Math. Theor. **54**, 105001 (2021).
- <sup>27</sup> W.-J. Rao, Physica A: Statistical Mechanics and its Applications **590**, 126689 (2022).
- <sup>28</sup> P. Sierant and J. Zakrzewski, Phys. Rev. B **99**, 104205 (2019).
- <sup>29</sup> W. Buijsman, V. Cheianov and V. Gritsev, Phys. Rev. Lett. **122**, 180601 (2019).
- <sup>30</sup> P. Sierant and J. Zakrzewski, Phys. Rev. B **101**, 104201 (2020).
- <sup>31</sup> A. D. Mirlin, Y. V. Fyodorov, F.-M. Dittes, J. Quezada, and T. H. Seligman, Phys. Rev. E **54**, 3221 (1996).
- <sup>32</sup> F. Evers and A. D. Mirlin, Phys. Rev. Lett. **84**, 3690 (2000).
- <sup>33</sup> A. D. Mirlin and F. Evers, Phys. Rev. B **62**, 7920 (2000).
- <sup>34</sup> F. Evers and A. D. Mirlin, Rev. Mod. Phys. **80**, 1355 (2008).
- <sup>35</sup> V. E. Kravtsov and K. A. Muttalib, Phys. Rev. Lett. **79**, 1913 (1997).
- <sup>36</sup> J. A. Méndez-Bermúdez, A. Alcazar-López, I. Varga, EPL **98**, 37006 (2012); J. Stat. Mech. P11012 (2014).

- <sup>37</sup> I. Varga, Phys. Rev. B **66**, 094201 (2002).
- <sup>38</sup> J. A. Méndez-Bermúdez and I. Varga, Phys. Rev. B **74**, 125114 (2006).
- <sup>39</sup> I. Varga and D. Braun, Phys. Rev. B **61**, 11859 (2000).
- <sup>40</sup> X. Cao, A. Rosso, J.-P. Bouchaud, and P. Le Doussal, Phys. Rev. E **95**, 062118 (2017).
- <sup>41</sup> V. Khemani, D. N. Sheng, and D. A. Huse, Phys. Rev. Lett. **119**, 075702 (2017).
- <sup>42</sup> M. Carrera-Núñez, A. M. Martínez-Argüello, J. A. Méndez-Bermúdez, Physica A: Statistical Mechanics and its Applications, **573**, 125965 (2021).
- <sup>43</sup> Y. Y. Atas, E. Bogomolny, O. Giraud, and G. Roux, Phys. Rev. Lett. **110**, 084101 (2013).
- <sup>44</sup> S. H. Tekur, U. T. Bhosale, and M. S. Santhanam, Phys. Rev. B **98**, 104305 (2018).
- <sup>45</sup> W.-J. Rao, Phys. Rev. B **102**, 054202 (2020).
- <sup>46</sup> J. M. G. Gomez, R. A. Molina, A. Relano, and J. Retamosa, Phys. Rev. E **66**, 036209 (2002).
- <sup>47</sup> F. Alet and N. Laflorencie, C. R. Physique **19**, 498-525 (2018).
- <sup>48</sup> P. Shukla, Phys. Rev. E **62**, 2098 (2000).
- <sup>49</sup> P. Shukla, Phys. Rev. E **75**, 051113 (2007).
- <sup>50</sup> D. N. Page, Phys. Rev. Lett. **71**, 1291 (1993).
- <sup>51</sup> L. Rademaker and M. Ortuño, Phys. Rev. Lett. **116**, 010404 (2016).
- <sup>52</sup> C. Monthus, Journal of Physics A: Mathematical and Theoretical **49**, 305002 (2016).
- <sup>53</sup> S. J. Thomson and M. Schiró, Phys. Rev. B **97**, 060201(R), (2018).
- <sup>54</sup> D. Pekker, B. K. Clark, V. Oganesyan, and G. Refael, Phys. Rev. Lett. **119**, 075701 (2017).
- <sup>55</sup> B. Bauer and C. Nayak, J. Stat. Mech. P09005 (2013).
- <sup>56</sup> D. E. Logan and S. Welsh, Phys. Rev. B **99**, 045131 (2019).
- <sup>57</sup> T. Papenbrock, Z. Pluhař, J. Tithof, and H. A. Weidenmüller, Phys. Rev. E **83**, 031130 (2011).
- <sup>58</sup> S. Pai, N. S. Srivatsa, and A. E. B. Nielsen, Phys. Rev. B **102**, 035117 (2020).
- <sup>59</sup> M. Haque, P. A. McClarty, I. M. Khaymovich, arXiv:2008.12782.
- <sup>60</sup> G. De Tomasi, I. M. Khaymovich, F. Pollmann, and S. Warzel, Phys. Rev. B **104**, 024202 (2021).
- <sup>61</sup> E. Bogomolny and M. Sieber, Phys. Rev. E **98**, 042116 (2018).
- <sup>62</sup> P. Nosov, I. M. Khaymovich, V. E. Kravtsov, Phys. Rev. B **99**, 104203 (2019).
- <sup>63</sup> G. De Tomasi and I. M. Khaymovich, Phys. Rev. Lett. **124**, 200602 (2020).
- <sup>64</sup> S.-X. Zhang and H. Yao, Phys. Rev. Lett. **121**, 206601 (2018).

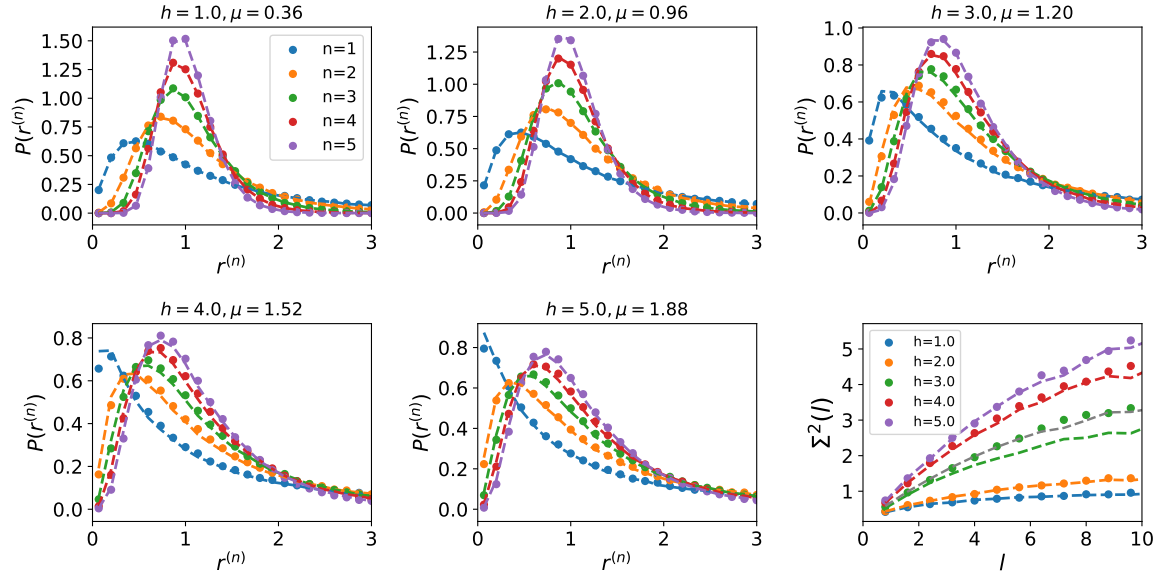


FIG. 5. The distributions of  $P(r^{(n)})$  in the orthogonal spin model without  $S_T^z$  conservation with comparisons to PRBM, the title of each sub-figure indicates the randomness strength  $h$  and fitted  $\mu$ . Bottom right:  $\Sigma^2(l)$  of the physical model and PRBM with  $\mu$  fitted through  $P(r^{(n)})$ , they fit quite well except for the transition region  $h \sim 3$ . Grey dashed line:  $\Sigma^2(l)$  of PRBM at  $\mu = 1.26$ . Dots and lines stand for physical data and PRBM in all cases.

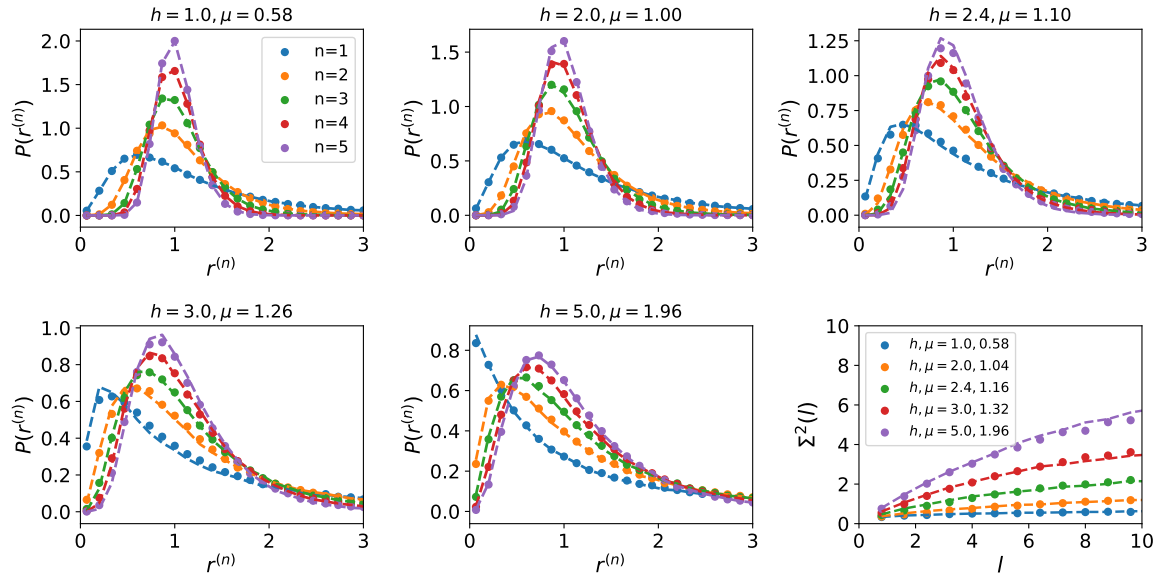


FIG. 6. The distributions of  $P(r^{(n)})$  in the unitary spin model without  $S_T^z$  conservation at various disorder strengths with comparisons to PRBM with  $\beta = 2$  and fitted  $\mu$ . Bottom right:  $\Sigma^2(l)$  of physical model and PRBM. Note here the values of  $\mu$  are fitted by  $\Sigma^2(l)$  as listed in the figure legend, they have minor deviations from those fitted through  $P(r^{(n)})$ , but the relative errors are controlled within 5%. Dots and lines stand for physical data and PRBM in all cases.